Investigation of 0^{+} states in ^{198}Hg after two-neutron pickup

C. Bernards, R. F. Casten, V. Werner, P. von Brentano, D. Bucurescu, G. Graw, S. Heinze, R. Hertenberger, J. Jolie, S. Lalkovski, D. A. Meyer, D. Mücher, P. Pejovic, C. Scholl, and H.-F. Wirth

Phys. Rev. C **87**, 024318 — Published 25 February 2013

DOI: 10.1103/PhysRevC.87.024318

Investigation of 0^+ states in ^{198}Hg after two-neutron pickup

C. Bernards*,[1] R.F. Casten,[1] V. Werner,[1] P. von Brentano,[2] D. Bucurescu,[3] G. Graw,[4] S. Heinze,[2] R. Hertenberger,[4] J. Jolie,[2] S. Lalkovski,[5] D.A. Meyer,[1] D. Mücher†,[2] P. Pejovic,[2] C. Scholl,[2] and H.-F. Wirth[6]

[1] *Wright Nuclear Structure Laboratory, Yale University, New Haven, CT-06520, USA*
[2] *Institut für Kernphysik, Universität zu Köln, D-50937 Köln, Germany*
[3] *National Institute for Physics and Nuclear Engineering, Bucharest, R-76900, Romania*
[4] *Fakultät für Physik, Ludwig-Maximilians-Universität München, D-85748 Garching, Germany*
[5] *Faculty of Physics, University of Sophia, 1164 Sofia, Bulgaria*
[6] *Physik Department, Technische Universität München, D-85748 Garching, Germany*

(Dated: February 13, 2013)

We studied 0^+ states in ^{198}Hg after the ^{200}Hg$(p,t)^{198}$Hg transfer reaction up to 3-MeV excitation energy. The experiment was performed using the high-resolution Q3D magnetic spectrograph at the Maier-Leibnitz Laboratory (MLL) Tandem accelerator in Munich. In total, only four 0^+ states were observed in ^{198}Hg, significantly fewer than in other experiments of the (p,t) transfer campaign. We discuss the low-energy 0^+ state density as a function of the valence nucleon number $N_{\rm val}$ and test if the 0^+ density can be used as a signature for the prolate-oblate shape-phase transition in the Hf-Hg region.

PACS numbers: 21.10.Re, 21.60.Ev, 25.40.Hs, 27.80.+w

I. INTRODUCTION

In recent years, much effort was invested in systematic studies of low-lying 0^+ excitations in medium- to heavy-mass nuclei throughout the nuclear landscape, ranging from ^{152}Gd to ^{194}Pt [1–5]. This region is particularly interesting, as the structure of these nuclei changes from transitional nuclei in the Gd region, over well-deformed nuclei in the Yb region, to γ-soft nuclei in the Pt region [6]. Experiments at the high-resolution Q3D magnetic spectrograph [7, 8] in Munich allowed the study of 0^+ states in unprecedented detail using (p,t) transfer reactions, and started with the discovery of an unforeseen high number of low-lying 0^+ excitations in ^{158}Gd [1]. Extending these studies to other nuclei, the enhanced density of low-lying 0^+ states in the Gd region was interpreted as a new signature for the shape-phase transitions from spherical to deformed nuclei [9]. These observations were followed by various calculations reproducing the density and distribution of 0^+ states [10–13].

These studies of 0^+ states were extended into the γ-soft region by investigating Pt isotopes [5]. The present work probes further towards the end of the proton and neutron shell. In the Hf-Hg region, a prolate-oblate phase transition has been observed by investigating several observables from ^{180}Hf to ^{200}Hg: energy ratios ($R_{4/2}$), quadrupole moments ($Q(2_1^+)$), and the reduced transition probabilities ($B(E2;2_2^+ \rightarrow 2_1^+)$) [14]. Extending the 0^+ studies to the Hg isotopes, we can test if the low-lying 0^+ density can be applied as a signature of this shape-phase transition as well.

*christian.bernards@yale.edu
†Present address: Physik Department, Technische Universität München, D-85748 Garching, Germany

II. EXPERIMENT

We performed a (p,t) transfer experiment at the Munich MLL (Maier-Leibnitz Laboratory of LMU Munich and TU Munich) Tandem accelerator facility using an unpolarized 25-MeV proton beam to impinge on a 48-μg/cm^2 ^{200}HgS target on a 7-μg/cm^2 carbon backing. The outgoing tritons were detected with the Q3D magnetic spectrograph [7] and the 1-m-long focal-plane detector [8] at three different laboratory angles with respect to the beam axis: 5°, 17.5°, and 30°, respectively. For every angle, two measurements with different magnetic settings were necessary to cover the excitation energy range of 0-3 MeV. The HgS target was highly enriched in ^{200}Hg (96.41%), and contained impurities of ^{201}Hg (1.46%), ^{199}Hg (0.99%), ^{202}Hg (0.91%), ^{198}Hg (0.13%), ^{204}Hg (0.10%), and ^{196}Hg (< 0.02%), respectively.

III. ANALYSIS AND RESULTS

The experimental setup allows straight-forward 0^+ state assignments using the data taken at 5° and 17.5°, since the (p,t) angular distribution strongly peaks in the forward direction only for the $L = 0$ transfer from the 0^+ ground state in ^{200}Hg to 0^+ states in ^{198}Hg [2]. Using this characteristic feature of the (p,t) angular distribution, it is sufficient to compare the ratio $R(5/17.5) \equiv \sigma(5°)/\sigma(17.5°)$ of the observed cross sections σ at these angles. The 30° data is not as significant for the determination of $L = 0$ transfers into ^{198}Hg, since it does not allow a clean separation of 0^+ states from 2^+ and 4^+ states [2]. However, the 30° data is very helpful as an additional data set for the identification of peaks and the spectra calibration. A safe lower limit for the $R(5/17.5)$ ratio, in order prevent incorrect assignments of 0^+ states, was previously chosen to be $R(5/17.5) > 3$ [4].

Figure 1 shows the complete triton spectrum for the 5° setting from 0 to 3 MeV. The data were calibrated using well-known excitation energies of ^{198}Hg states. We normalized all experimental runs (different angles and magnetic settings) to the integrated beam current measured behind the target. In Fig. 1, the intensity of the high-energy (HE) part, colored in green, is normalized to the low-energy (LE) part. Due to the high resolving power (4-6 keV FWHM for 15 to 20-MeV tritons) of the Q3D setup and focal plane detector, a total of ~ 70 excited states were analyzed in this work. Figure 2 illustrates the differences between spectra taken at 5° and 17.5°, the relevant angles for the assignment of 0^+ states. Levels corresponding to ^{198}Hg and peaks arising from target impurities are labeled in the plot. Contaminants from target impurities were identified by comparison with the Q values of the corresponding (p,t) transfer reaction.

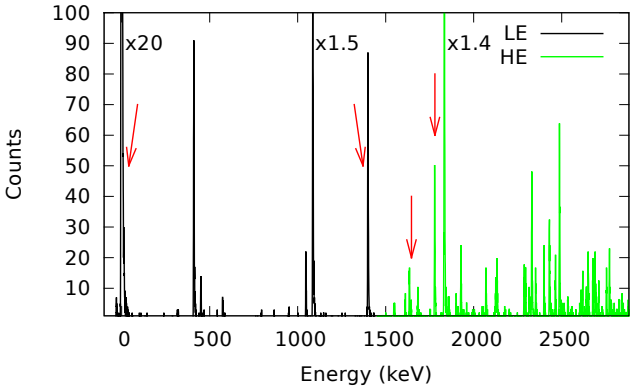

FIG. 1: (Color online) Plot of the complete triton spectrum from 0 to $\sim$ 3 MeV, measured at 5° laboratory angle. The intensity of the high-energy (HE) part of the spectrum is normalized to the low-energy (LE) part. The arrows mark the assigned 0^+ states in ^{198}Hg. The 1646-keV 0^+ state is not visible in this plot due to its small cross section.

The $R(5/17.5)$ ratios – for all observed states that were not identified as contaminants – are plotted in Fig. 3. The threshold $R(5/17.5) = 3$ is marked by a green horizontal line. In total, we observed only four states that exceed this limit and we discuss these states below.

Table I lists the observed states that exceed the $R(5/17.5) = 3$ limit seen in Fig. 3. Besides the ground state, we observe three more states showing this typical $L = 0$ transfer characteristic. Two of these states, the 0^+ states at 1401 and 1780 keV, are already known and assigned as 0^+ states [15, 16]. In addition, we found a new, weakly populated state at 1646 keV. We only observe a

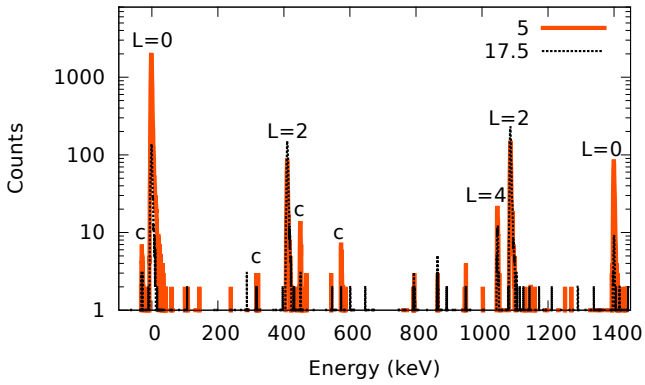

FIG. 2: (Color online) Logarithmic plot comparing the 5° and the normalized 17.5° spectra for the LE setting. States identified as ^{198}Hg states are labeled with the corresponding transfer $L = 0, 2,$ or 4 from the ^{200}Hg ground state. Identified contaminants are labeled with **c**. They correspond to excited or ground states in ^{199}Hg, ^{200}Hg, ^{197}Hg, and ^{196}Hg.

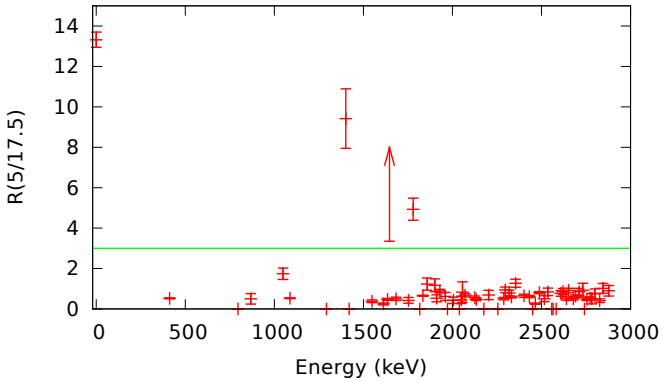

FIG. 3: (Color online) $R(5/17.5)$ ratio used to identify 0^+ states in ^{198}Hg. The green line marks the $R(5/17.5) = 3$ threshold that is used as a lower limit for 0^+ assignments.

peak of that energy in the 5° data. By carefully testing our detection sensitivity in the 17.5° spectrum, we derive an upper limit for the 17.5° cross section and consequentially give a lower limit for the $R(5/17.5)$ ratio. With 3.35, this lower limit is clearly distinguishable from all other observed states that do not correspond to a $L = 0$ transfer. Since we have the isotopic analysis on the target purity and were able to identify peaks originating from the most significant impurities in the spectra, we believe that this state does not stem from a target impurity and corresponds to a 0^+ excitation in ^{198}Hg. In Ref. [16], a further 0^+ state was assigned at 1550 keV, as well, based on a (p,t) transfer experiment. We observe a state at 1549 keV, but our much higher resolution data does not support this 0^+ assignment since $R(5/17.5) \approx 0.4$. Our result is consistent with the $\gamma\gamma$ angular correlation data of Ref. [17].

TABLE I: $R(5/17.5)$ ratios and cross sections of assigned 0^+ states, discussed in detail in the text.

Energy (keV)	$R(5/17.5)$	$\sigma(5°)$ (mb/sr)	$\sigma(17.5°)$ (mb/sr)
0.0 (0)	13.32 (38)	0.7956 (798)	0.0597 (62)
1401.0 (3)	9.42 (147)	0.0225 (25)	0.0024 (4)
1646.4 (8)	>3.35	0.0009 (3)	<0.0002
1779.6 (2)	4.93 (55)	0.0145 (17)	0.0029 (4)

A summary of all observed states and their cross sections for all measured angles is given in Table II. The listed absolute cross sections include a 10% error from the beam-current normalization on the target. In case of very weakly-excited states, such as the 0^+ state at 1646 keV, we were not always able to measure the cross sections for all three angles if it was below our detection sensitivity. Nevertheless, none of the other weakly excited states seems to correspond to a $L = 0$ transfer in ^{198}Hg. The origin of the low-intensity peaks at 796 and 867 keV is not clear. However, considering the fact that they would correspond to the second and third excited state in ^{198}Hg, we assume that they most likely stem from unidentified contaminants.

In order to rule out the possibility that the low number of observed $L = 0$ transfers in this experiment is simply limited by statistics, we compare our measured cross sections with cross sections from other already analyzed experiments of this Q3D (p, t) campaign. The 0^+ state at 1646 keV is the weakest excited 0^+ state we observe in ^{198}Hg. The cross section $\sigma(5°) = 0.0009$ mb/sr is very similar to the absolute cross sections $\sigma(5°)$ for the weakest populated 0^+ states observed in Refs. [2, 5]. With $\sigma(5°) = 0.0009$ mb/sr, the cross section of the 0^+ state at 1646 keV is about 0.1% of the ground-state cross section at 5°. This variation in excitation cross sections is in good agreement with the variation of cross sections reported in Ref. [5], where the least populated assigned 0^+ states in ^{192}Pt and ^{194}Pt have about 0.1-0.2% of the ground-state cross section measured at 5° laboratory angle. Therefore, we conclude that the sensitivity to identify 0^+ states in this data set is similar to the sensitivity of other experiments performed within this (p, t) campaign [2, 4, 5].

TABLE II: Summary of observed peaks and their cross sections. The cross sections have a 10% systematic uncertainty due to the beam-current normalization. The uncertainties on the relative $R(5/17.5)$ ratios are often smaller.

	Cross section (mb/sr)		
Energy (keV)	$\sigma(5°)$	$\sigma(17.5°)$	$\sigma(30°)$
-28.4 (3) [†]	0.0024 (4)	0.0007 (3)	0.0018 (5)
0.0 (0) [∗]	0.7956 (798)	0.0597 (62)	0.4052 (409)
322.3 (7) [†]	0.0007 (3)	0	0.0010 (5)
411.7 (2) [∗]	0.0286 (31)	0.0548 (57)	0.0364 (40)
451.6 (3) [†]	0.0038 (6)	0.0007 (3)	0.0022 (6)
575.6 (4) [†]	0.0018 (4)	0	0.0007 (4)
795.9 (8) [‡]	0	0.0007 (3)	0
867.4 (6) [‡]	0.0005 (2)	0.0009 (3)	0
1048.7 (2) [∗]	0.0056 (8)	0.0032 (5)	0.0029 (6)
1087.8 (1) [∗]	0.0368 (39)	0.0692 (71)	0.0546 (59)
1292.4 (11)	0	0.0004 (2)	0
1401.0 (3) [∗]	0.0225 (25)	0.0024 (4)	0.0054 (9)
1419.9 (9)	0	0	0.0006 (2)
1548.6 (2)	0.0019 (4)	0.0051 (6)	0.0062 (7)
1612.3 (2) [∗]	0.0021 (4)	0.0085 (10)	0.0041 (5)
1635.7 (1) [∗]	0.0057 (8)	0.0122 (13)	0.0183 (19)
1646.4 (8)	0.0009 (3)	<0.0002	0
1683.3 (1) [∗]	0.0029 (5)	0.0058 (7)	0.0110 (12)
1752.8 (3)	0.0008 (3)	0.0020 (3)	0.0026 (4)
1779.6 (2)	0.0145 (17)	0.0029 (4)	0.0092 (10)
1816.2 (4)	0	0.0006 (2)	0.0011 (2)
1834.4 (2)	0.0474 (50)	0.0726 (74)	0.0835 (85)
1901.3 (4)	0.0014 (3)	0.0012 (2)	0.0017 (3)
1911.0 (3)	0.0009 (3)	0.0017 (3)	0.0033 (4)
1929.1 (2) [∗]	0.0078 (10)	0.0088 (10)	0.0077 (9)
1960.2 (4)	0.0009 (3)	0.0015 (3)	0.0025 (4)
1971.9 (7)	0	0.0001 (1)	0.0008 (2)
2005.8 (3)	0.0007 (3)	0.0018 (3)	0.0014 (3)
2038.9 (8)	0	0.0006 (2)	0
2049.8 (7)	0.0007 (3)	0.0015 (3)	0.0012 (2)
2056.2 (9)	0.0008 (3)	0.0009 (5)	0.0004 (2)
2071.3 (2) [∗]	0.0047 (7)	0.0069 (8)	0.0032 (4)
2125.7 (2)	0.0031 (5)	0.0057 (7)	0.0076 (9)
2134.2 (2)	0.0055 (8)	0.0120 (13)	0.0104 (12)
2176.6 (22)	0	0.0007 (2)	0.0005 (2)
2203.4 (4)	0.0008 (3)	0.0012 (2)	0.0015 (3)
2254.6 (6)	0	0	0.0011 (2)
2287.9 (2)	0.0050 (7)	0.0099 (11)	0.0061 (7)
2296.3 (2)	0.0040 (6)	0.0042 (6)	0.0044 (6)
2318.6 (10)	0.0024 (4)	0.0030 (4)	0.0051 (6)
2331.3 (1) [∗]	0.0114 (13)	0.0195 (21)	0.0346 (36)
2354.5 (7)	0.0035 (5)	0.0027 (4)	0.0056 (7)
2401.1 (2)	0.0046 (7)	0.0071 (8)	0.0076 (9)
2431.5 (1)	0.0084 (10)	0.0138 (15)	0.0207 (22)
2450.4 (8)	0	0.0006 (2)	0
2465.5 (2)	0.0044 (6)	0.0171 (19)	0.0117 (13)
2488.6 (2)	0.0149 (17)	0.0186 (20)	0.0173 (19)
2516.2 (2)	0.0010 (3)	0.0020 (3)	0.0033 (5)
2535.8 (3)	0.0018 (4)	0.0021 (4)	0.0026 (4)
2557.6 (5)	0	0.0021 (3)	0.0032 (4)
2564.9 (7)	0	0.0008 (2)	0
2582.1 (7)	0	0.0007 (2)	0.0006 (2)
2608.5 (15)	0.0022 (4)	0.0029 (4)	0.0033 (5)
2620.3 (3)	0.0027 (5)	0.0031 (4)	0.0041 (5)
2640.1 (6)	0.0026 (4)	0.0051 (7)	0.0047 (6)
2651.7 (3)	0.0054 (7)	0.0059 (7)	0.0076 (9)
2678.5 (3)	0.0039 (6)	0.0077 (9)	0.0063 (8)
2691.3 (3)	0.0044 (6)	0.0070 (8)	0.0147 (16)
2711.3 (3)	0.0021 (4)	0.0025 (4)	0.0033 (5)
2731.5 (4) [∗]	0.0008 (2)	0.0008 (2)	0.0012 (2)
2741.1 (7)	0	0.0006 (2)	0
2755.2 (4)	0.0037 (6)	0.0078 (9)	0.0106 (12)
2772.4 (3)	0.0054 (7)	0.0099 (11)	0.0111 (13)
2782.5 (7)	0.0018 (9)	0.0035 (4)	0.0031 (5)
2800.5 (5)	0.0009 (2)	0.0011 (2)	0.0020 (3)
2826.3 (5)	0.0015 (3)	0.0036 (5)	0.0041 (5)
2844.7 (4)	0.0016 (3)	0.0016 (3)	0.0018 (3)
2877.5 (13)	0.0011 (3)	0.0012 (2)	0.0007 (2)

[∗] This state was used for energy calibration using the published ^{198}Hg excitation energy from the data sheets [15].
[†] Identified contaminant from target impurity.
[‡] Very likely an unidentified contaminant.

IV. DISCUSSION

With the investigation of ^{198}Hg, we extend our search for 0^+ states from the rare-earth region towards the ^{208}Pb shell closure. The density of low-energy 0^+ states differs for the different nuclei investigated in this (p,t) campaign and is shown in histogram form in Fig. 4. With only four assigned 0^+ states up to 3 MeV excitation, ^{198}Hg clearly has the lowest number of low-energy 0^+ states among the investigated nuclei. In Fig. 4, the nuclei ^{154}Gd, ^{194}Pt and ^{198}Hg are highlighted. Their position in the graph is particularly interesting when interpreting the 0^+ density as a signature for shape-phase transitions. In Ref. [9], the large number of low-lying 0^+ states in ^{154}Gd was interpreted as a signature for the shape-phase transition from spherical to deformed nuclei, with ^{154}Gd being closest to the critical point.

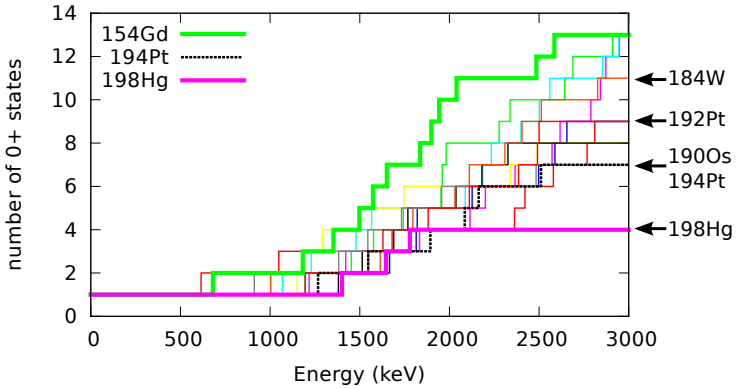

FIG. 4: (Color online) Histogram of the cumulative number of definite 0^+ states up to 3-MeV excitation energy using the results of 13 different Q3D (p,t) experiments. Plotted are the definite 0^+ assignments for ^{152}Gd, ^{154}Gd, ^{158}Gd, ^{162}Dy, ^{168}Er, ^{170}Yb, ^{176}Hf, ^{180}W, ^{184}W, ^{190}Os, ^{192}Pt, ^{194}Pt, and ^{198}Hg. The data for the different nuclei is taken from Refs. [1–5] and the present work. The enveloping lines for the 0^+ states in ^{154}Gd and ^{198}Hg – and the nucleus ^{194}Pt – are highlighted. Nuclei in the $A \approx 190$ - 200 mass region investigated in Ref. [14] are labeled on the right-hand side of the graph.

Now, having data available on ^{198}Hg from a comparably sensitive experiment, we can test how the 0^+ density evolves at the prolate-oblate phase-shape transition observed in the Hf-Hg region [14]. For this shape-phase transition, it was concluded that the nucleus ^{194}Pt is closest to the critical point.

The corresponding mass $A \approx 190$ - 200 nuclei and their 0^+ state densities are marked by arrows in Fig. 4. Their evolution does not show an enhancement in ^{194}Pt. The 0^+ density seems to depend rather on the proximity of the ^{208}Pb shell closure. Indeed, ^{198}Hg has the fewest number of 0^+ states. This behavior seems to be a simple consequence of the number of configurations available to create 0^+ states. This number decreases rapidly as the closed shell at ^{208}Pb is approached.

The Interacting Boson Model (IBM) [18] has turned out to be very useful for the description of collective properties of nuclei by using a simple Hamiltonian, only considering valence nucleons (holes), and treating them pairwise as bosons. Using the *sd* IBM-1 version of the model, only spin $l = 0$ or $l = 2$ bosons are considered and no distinction between protons or neutrons is made. Thus, the $N_{\rm val}$ valence nucleons are approximated by $N_{\rm val}/2$ *sd* bosons. The decrease in the number of 0^+ states in Fig. 4 is in qualitative agreement with IBM calculations performed for these nuclei [10]. We investigate this further in Fig. 5.

In Fig. 5 we plot the number of 0^+ state assignments up to 3 MeV as a function of the number of valence nucleons (holes) $N_{\rm val}$. Tentative assignments are accounted for in the upper error bars. In addition, we show the total number of 0^+ states that can be formed within the *sd* IBM-1. By comparing this maximum number of IBM 0^+ states with the number of observed 0^+ states, one notes an upward trend, similar in the data and calculations, up to $N_{\rm val} \sim 22$ valence nucleons, corresponding to ^{154}Gd. The total number of low-lying 0^+ states for the individual nuclei, as well as the increasing number of 0^+ states with $N_{\rm val}$ are reasonably reproduced. Of course, the IBM is a highly truncated model that includes only a small part of the full shell-model space. Moreover, some of the IBM 0^+ states may well lie above 3 MeV so one would expect

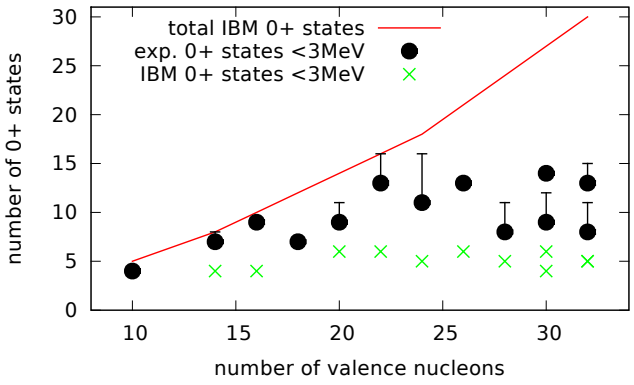

FIG. 5: (Color online) Number of 0^+ states up to 3 MeV for the nuclei investigated in this Q3D (p,t) campaign as a function of the number of valence nucleons $N_{\rm val}$. The error bars include tentative assignments. In addition, the maximum number of *sd* IBM 0^+ states and the calculated number of 0^+ states below 3 MeV in this model using realistic parameters fitted according to Refs. [20, 21] are plotted.

to observe only a subset of the possible configurations and states in the calculation. Thus, one should view the concordance in the number of 0^+ states in the IBM and the experimentally observed ones up to $N_{\rm val} \sim 22$ only in a qualitative way as indicating the general trends and the rapid increase in the number of allowed 0^+ configurations.

Above $N_{\rm val} \sim 22$ the number of experimentally observed low-lying 0^+ states tends to saturate and is relatively constant, taking uncertainties due to tentative assignments into account. For $N_{\rm val} > 22$, even the truncated number of IBM 0^+ states far exceeds the number seen experimentally. In strong contrast to the maximum number of 0^+ states in the *sd* IBM space, we plot the number actually calculated to lie below 3 MeV in the IBM using realistic parameters and the extended consistent Q formalism [19] as in Refs. [20, 21]. The parameters were fitted to a number of key observables in the ground, 0_2^+, and quasi-2_γ^+ band by considering contour plots [20–22]. For the energies, emphasis was placed on the ratios $R_{4/2} = E(4_1^+)/E(2_1^+)$, $E(0_2^+)/E(2_1^+)$, and $E(2_\gamma^+)/E(2_1^+)$. For electro-magnetic transition probabilities, the $B(E2)$ ratios $B_{2\gamma} = B(E2;2_\gamma^+ \rightarrow 0_1^+)/B(E2;2_1^+ \rightarrow 0_1^+)$ and $R_{2\gamma} = B(E2;2_\gamma^+ \rightarrow 0_1^+)/B(E2;2_\gamma^+ \rightarrow 2_1^+)$ were considered. The resulting parameters were found to allow a realistic description of the 0_2^+ level energies [20] and are now used to calculate the low-energy 0^+ states up to 3-MeV excitation energy. The calculated 0^+ densities below 3 MeV do not show an increase in the number of 0^+ states with $N_{\rm val}$ and result in a rather constant number (4 - 6) of 0^+ states in the energy range investigated, similar to the experimentally observed saturation, but naturally with fewer states than observed. This hints at the fact that the number of experimentally observed 0^+ states includes many non-collective 0^+ states which are not described in the IBM. The data shown in Fig. 5 are listed in Table III.

The overall conclusion from Fig. 5 is the strong increase in the number of observed low-lying 0^+ states as the valence space expands, followed by a saturation in this number near mid-shell. These features should be characteristic of any realistic theoretical interpretation of these results.

TABLE III: Investigated nuclei plotted in Fig. 5 sorted by their number of valence nucleons $N_{\rm val}$. The numbers of 0^+ states correspond to states up to 3-MeV excitation energy.

Nucleus:	^{198}Hg	^{194}Pt	^{192}Pt	^{190}Os	^{152}Gd	^{154}Gd	^{184}W	^{158}Gd	^{180}W	^{162}Dy	^{170}Yb	^{168}Er	^{176}Hf
$N_{\rm val}$:	10	14	16	18	20	22	24	26	28	30	30	32	32
Exp. 0^+ states:	4	7	9	7	9	13	11	13	8	9	14	13	8
Calc. 0^+ states:		4	4		6	6	5	6	5	4	6	5	5

V. CONCLUSION

To summarize, in a high-resolution experiment at the Tandem accelerator at LMU and TU Munich, we have identified the 0^+ states in ^{198}Hg up to about 3 MeV, finding far fewer than in other investigated nuclei. We note that recent experiments [5] on ^{194}Pt and ^{192}Pt show more 0^+ states than ^{198}Hg but fewer than in the nuclei near mid-shell. Thus, there is an approximately linear increase in the number of 0^+ states below 3 MeV as a function of valence-nucleon number up to about 22 valence nucleons. This is reasonable due to the increasing number of possible 0^+ shell-model configurations. However, a second, contrasting, feature of the data is a saturation in the number of low-lying 0^+ states as one goes

further into the shell (larger numbers of valence nucleons). This runs counter to the obvious increase in the total number of available 0^+ configurations with increasing valence-space size and is most likely due to the fact that many of the allowed 0^+ configurations lie well above 3 MeV in excitation energy.

VI. ACKNOWLEDGMENTS

We thank the operators at MLL for excellent beam conditions. This research has been supported by the US DOE under Grant No. DE-FG02-91ER-40609, MLL, DFG Grant No. C4-Gr894/2-3, and the Romanian UEFISCDI project PN-II-ID-PCE-2011-3-0140.

[1] S.R. Lesher, A. Aprahamian, L. Trache, A. Oros-Peusquens, S. Deyliz, A. Gollwitzer, R. Hertenberger, B.D. Valnion, and G. Graw Phys. Rev. C **66**, 051305(R) (2002).

[2] D.A. Meyer, V. Wood, R.F. Casten, C.R. Fitzpatrick, G. Graw, D. Bucurescu, J. Jolie, P. von Brentano, R. Hertenberger, H.-F. Wirth, N. Braun, T. Faestermann, S. Heinze, J.L. Jerke, R. Krücken, M. Mahgoub, O. Möller, D. Mücher, and C. Scholl Phys. Rev. C **74**, 044309 (2006).

[3] D. Bucurescu, G. Graw, R. Hertenberger, H.-F. Wirth, N. Lo Iudice, A.V. Sushkov, N.Yu. Shirikova, Y. Sun, T. Faestermann, R. Krücken, M. Mahgoub, J. Jolie, P. von Brentano, N. Braun, S. Heinze, O. Möller, D. Mücher, C. Scholl, R.F. Casten, and D.A. Meyer, Phys. Rev. C **73**, 064309 (2006).

[4] L. Bettermann, S. Heinze, J. Jolie, D. Mücher, O. Möller, C. Scholl, R.F. Casten, D.A. Meyer, G. Graw, R. Hertenberger, H.-F. Wirth, and D. Bucurescu, Phys. Rev. C **80**, 044333 (2009).

[5] G. Ilie, R.F. Casten, P. von Brentano, D. Bucurescu, T. Faestermann, G. Graw, S. Heinze, R. Hertenberger, J. Jolie, R. Krücken, D.A. Meyer, D. Mücher, C. Scholl, V. Werner, R. Winkler, and H.-F. Wirth, Phys. Rev. C **82**, 024303 (2010).

[6] P. Cejnar, J. Jolie, and R.F. Casten, Rev. Mod. Phys. **82**, 2155 (2010).

[7] M. Löffler, H.J. Scheerer, and H. Vonach, Nucl. Instr. Methods **111**, 1 (1973).

[8] H.-F. Wirth, Ph.D. thesis, Technische Universität München, 2001 [`http://tumb1.biblio.tu-muenchen.de/publ/diss/ph/2001/wirth.html`].

[9] D.A. Meyer, V. Wood, R.F. Casten, C.R. Fitzpatrick, G. Graw, D. Bucurescu, J. Jolie, P. von Brentano, R. Hertenberger, H.-F. Wirth, N. Braun, T. Faestermann, S. Heinze, J.L. Jerke, R. Krücken, M. Mahgoub, O. Möller, D. Mücher, and C. Scholl, Phys. Lett. **B638**, 44 (2006).

[10] N.V. Zamfir, Jing-ye Zhang, and R.F. Casten, Phys. Rev. C **66**, 057303 (2002).

[11] Yang Sun, Ani Aprahamian, Jing-ye Zhang, and Ching-Tsai Lee, Phys. Rev. C **68**, 061301(R) (2003).

[12] N. Lo Iudice, A.V. Sushkov, and N.Yu. Shirikova, Phys. Rev. C **70**, 064316 (2004).

[13] N. Lo Iudice, A.V. Sushkov, and N.Yu. Shirikova, Phys. Rev. C **72**, 034303 (2005).

[14] J. Jolie and A. Linnemann, Phys. Rev. C **68**, 031301(R) (2003).

[15] Z. Chunmei, Nuclear Data Sheets **95**, 59 (2002).

[16] M. Vergnes, G. Berrier-Ronsins, G. Rotbard, J. Skalski, and W. Nazarewicz, Nucl. Phys. **A514**, 381 (1990).

[17] C. Bernards, S. Heinze, J. Jolie, C. Fransen, A. Linnemann, and D. Radeck, Phys. Rev. C **79**, 054307 (2009).

[18] F. Iachello and A. Arima, *The Interacting Boson Model* (Cambridge University Press, Cambridge, UK, 1987).

[19] P.O. Lipas, P. Toivonen, and D.D. Warner, Phys. Lett. **B155**, 295 (1985).

[20] E.A. McCutchan, N.V. Zamfir, and R.F. Casten, Phys. Rev. C **69**, 064306 (2004).

[21] E.A. McCutchan and N.V. Zamfir, Phys. Rev. C **71**, 054306 (2005).

[22] W.-T. Chou, N.V. Zamfir, and R.F. Casten, Phys. Rev. C **56**, 829 (1997).